Long-term acupuncture treatment has a multi-targeting regulation on multiple brain regions in rats with Alzheimer's disease: a positron emission tomography study

Yang-jia Lu[1, 2, #], Xiao-wen Cai[1, #], Gui-feng Zhang[3, #], Yong Huang[1, *], Chun-zhi Tang[4, *], Bao-ci Shan[5], Shao-yang Cui[4, 6], Jun-qi Chen[7], Shan-shan Qu[1], Zheng Zhong[1], Xin-sheng Lai[4], Genevieve Zara Steiner[8]

1 School of Traditional Chinese Medicine, Southern Medical University, Guangzhou, Guangdong Province, China
2 Traditional Chinese Medicine of the Second Clinical School, Guangdong Medical College, Dongguan, Guangdong Province, China
3 Zhaoqing Medical College, Zhaoqing, Guangdong Province, China
4 Clinical Medical College of Acupuncture, Moxibustion and Rehabilitation, Guangzhou University of Chinese Medicine, Guangzhou, Guangdong Province, China
5 Key Laboratory of Nuclear Analytical Techniques, Institute of High Energy Physics, Chinese Academy of Sciences, Beijing, China
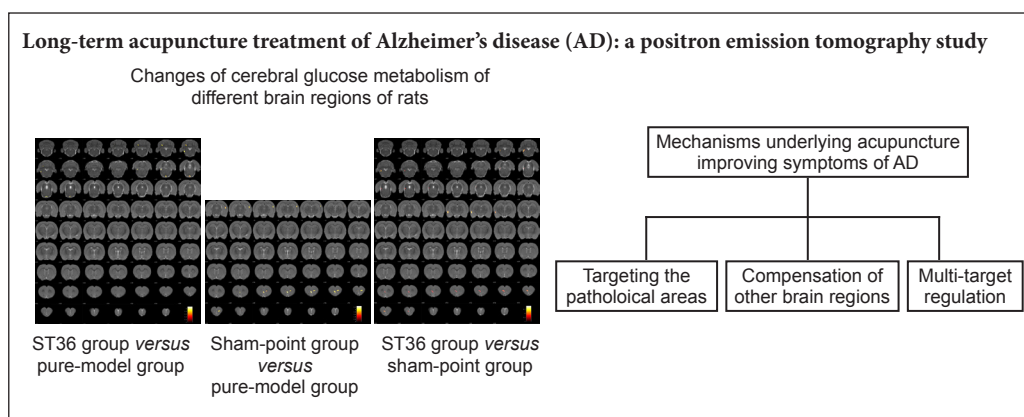6 Shenzhen Hospital of Guangzhou University of Chinese Medicine, Shenzhen, Guangdong Province, China
7 Huarui Hospital of Southern Medical University, Guangzhou, Guangdong Province, China
8 National Institute of Complementary Medicine, Western Sydney University, Penrith NSW, Australia

Graphical Abstract

Long-term acupuncture treatment of Alzheimer's disease (AD): a positron emission tomography study

Changes of cerebral glucose metabolism of different brain regions of rats

ST36 group *versus* pure-model group

Sham-point group *versus* pure-model group

ST36 group *versus* sham-point group

Mechanisms underlying acupuncture improving symptoms of AD

Targeting the patholoical areas | Compensation of other brain regions | Multi-target regulation

Correspondence to:
Yong Huang, Ph.D. or
Chun-zhi Tang, Ph.D.,
nanfanglihuang@163.com or
jordan664@163.com.

#These authors contributed equally to this study.

orcid:
0000-0003-2652-8586
(Yong Huang)
0000-0003-3127-578X
(Chun-zhi Tang)

Abstract

The acute effect of acupuncture on Alzheimer's disease, *i.e.*, on brain activation during treatment, has been reported. However, the effect of long-term acupuncture on brain activation in Alzheimer's disease is unclear. Therefore, in this study, we performed long-term needling at *Zusanli* (ST36) or a sham point (1.5 mm lateral to ST36) in a rat Alzheimer's disease model, for 30 minutes, once per day, for 30 days. The rats underwent ^{18}F-fluorodeoxyglucose positron emission tomography scanning. Positron emission tomography images were processed with SPM2. The brain areas activated after needling at ST36 included the left hippocampus, the left orbital cortex, the left infralimbic cortex, the left olfactory cortex, the left cerebellum and the left pons. In the sham-point group, the activated regions were similar to those in the ST36 group. However, the ST36 group showed greater activation in the cerebellum and pons than the sham-point group. These findings suggest that long-term acupuncture treatment has targeted regulatory effects on multiple brain regions in rats with Alzheimer's disease.

Key Words: nerve regeneration; neurodegeneration; acupuncture; Zusanli (ST36); Alzheimer's disease; long-term treatment; positron emission tomography; rat; mechanism; targeting effect; compensation; multi-target regulation; neural regeneration

Introduction

Alzheimer's disease (AD) is characterized by progressive memory loss and cognitive dysfunction. Recently, acupuncture is playing an increasingly greater complementary role in treating AD. Researchers have shown that acupuncture is safe and effective and that it can improve cognition and overall functioning, thereby improving the quality of life of AD patients (Simoncini et al., 2015; Zhou et al., 2015; Zhang et al., 2016). However, the mechanisms underlying the therapeutic effects of acupuncture in AD remain unclear.

A striking feature of AD is glucose hypometabolism in brain regions related to cognition. Reductions in glucose metabolism are found in the hippocampus, bilateral precuneus and the posterior cingulate, and are correlated with symptom severity and functional decline in patients (Dukart et al., 2013; Roy et al., 2014). These changes are also seen in cognitively normal patients with AD (Lai et al., 2015; Tahmasian et al., 2015). Furthermore, in animal models, ^{18}F-fluorodeoxyglucose (FDG) uptake is lower in several brain regions, such as the olfactory bulb, hippocampus and cerebral cortex, observed by our research group (Lu et al., 2015). These findings are similar to those of Xiao et al. (2015). Therefore, in the present study, we examined cerebral glucose metabolism in the brain using ^{18}F-FDG positron emission tomography (PET) in a rat model of AD.

Acupuncture has been demonstrated to have a beneficial effect on cognitive impairment (Li et al., 2016). Our previous studies in the rat showed that acupuncture increases blood perfusion and glucose metabolism in various brain regions, including the pyriform cortex of the left and right limbic systems, the olfactory cortex of the left and right temporal lobes, the right amygdaloid body, and the right hippocampus (Lu et al., 2014; Lai et al., 2015).

Our present study has a number of unique features. First, only one acupoint, *Zusanli* (ST36), was chosen for treatment. According to traditional Chinese medicine theory, a deficiency of spleen and stomach is the fundamental cause of AD. ST36 is an acupoint of the Stomach Meridian of Foot-*Yangming*, and plays an essential role in regulating the function of the spleen and stomach. In our previous report, we performed a preliminary study of acupuncture at ST36 and a non-acupoint (Lu et al., 2014). In the present study, we combined acupuncture at ST36 with PET for a clearer observation of acupuncture's mechanism of action.

AD requires a long-term treatment because of the progressive neurodegenerative changes. Another study focused on *Shenmen* (HT7) and showed that acupuncture at HT7 effects cerebral glucose metabolism after a 30-day treatment (Lai et al., 2015). Both ST36 and HT7 are commonly used acupoints for the treatment of AD. Hence, in the current study, a 30-day treatment regimen was used with ^{18}F-FDG PET to further explore the mechanism of long-term acupuncture treatment at ST36 in a rat model of AD. Different from the previous studies which mostly focused on only one mechanism, the study hypothesized that acupuncture treated AD from several aspects.

Materials and Methods

Experimental animals

Seventy-five 2-month-old Sprague-Dawley rats (38 males and 37 females) weighing 200–250 g were provided by the Animal Center of China Academy of Chinese Medical Sciences (Beijing, China; license No. SCXK (Jing) 2011-0007). The study protocol was approved by the Ethics Committee of Guangzhou University of Chinese Medicine (No. SPF20110032). The experimental procedure followed the the United States National Institutes of Health Guide for the Care and Use of Laboratory Animals (NIH Publication No. 85-23, revised 1986), and "Consensus Author Guidelines on Animal Ethics and Welfare" produced by the International Association for Veterinary Editors (IAVE).

AD model establishment

Several studies have shown the feasibility of intraperitoneal injection of D-galactose (Shanghai No. 2 Reagent Company, Shanghai, China) combined with injection of ibotenic acid (Sigma-Aldrich, St. Louis, MO, USA) into the basal nuclei to generate a rat model of AD (Budni et al., 2016; Karthick et al., 2016). D-galactose accelerates the natural aging process, which contributes to the pathogenesis of AD. Ibotenic acid impairs the long-term memory of rats.

The 75 rats were housed in separate cages with controlled illumination (12-hour light/dark cycle), humidity and temperature (18–22°C). The rats were randomly divided into a normal group (*n* = 15; 8 males, 7 females) and a pre-model group (*n* = 60; 30 males, 30 females). The latter group received 0.96% D-galactose (prepared in 0.9% saline; Guangxi Nanning Baihui Pharmaceutical Group Co., Ltd., Nanning, China) by intraperitoneal injection (5 mL/kg) every day for 6 weeks. After that, the rats in the pre-model group were anesthetized and placed in a stereotaxic apparatus (Xi'an Northwest Photoelectric Instrument Factory, Xi'an, China), given a slow injection of 1 μL 5 μg/μL ibotenic acid (prepared in 0.9% saline) into both sides of the brain. The syringe was left in place for 10 minutes after the 10-minute injection (Zhong et al., 2005a, b). Two weeks later, 15 rats (7 males, 8 females) in the pre-model group died in the procedure. The remaining 45 rats in this group were equally and randomly divided into the following three groups: model group (7 males, 8 females), ST36 group (8 males, 7 females) and sham-point group (7 males, 8 females). The ST36 group and sham-point group then received a 30-day acupuncture treatment. The normal and model groups served as control groups, receiving no acupuncture treatment.

ST36 and sham point locations

ST36 is located 5 mm directly below the capitulum fibulae, according to *Acupoint Location for Experimental Animals* (Hu, 2003). Based on a previous study (Lin et al., 2013), the selected sham point is 1.5 mm distal to the ST36 point. In this experiment, we used points on the right side of the rats.

Acupuncture treatment

The treatment continued for 30 days (Lai et al., 2015). Each rat was acupunctured once per day at the Experimental Animals Center of the China Academy of Chinese Medical Sci-

ences from 08:00 to 12:00, and each single needling session lasted for almost 30 minutes. After the overlying skin was sterilized, sterile acupuncture needles (0.18 mm in diameter and 9 mm in length, manufactured by the Beijing Zhongyan Taihe Medical Instrument Co., Ltd., Beijing, China) were inserted perpendicularly into the ST36 point or sham-point to a depth of approximately 3 mm with uniform twisting, lifting and thrusting. Each needling lasted for 30 minutes and was performed once per day. After the 30-day treatment period, the rats (including the healthy control and pre-model rats) were subjected to the Y-maze test and ^{18}F-FDG-PET imaging.

Y-maze test

Learning and memory abilities were tested using the Y-maze test system (Zhenhua Teaching Instrument Factory, Yuanyang, China). A correct response was noted only if the rat directly moved into the secure arm of the Y-maze when it received a foot shock (0.6 mA). The rats were trained until they had reached the learning criterion; namely, having 9 correct responses within 10 consecutive training trials. The Y-maze test results were calculated as the time required by the rats to reach the learning criterion. The shorter the time required for training, the greater the capacity for learning. The tests were carried out by professionals in a quiet and dim room, with a fixed training time.

^{18}F-FDG-PET imaging

On day 31, all of the rats were sent to the PET-CT Center of the Experimental Animals Center of the No. 301 Chinese People's Liberation Army General Hospital after 24 hours of fasting. The rats underwent the following procedure: (1) The blood sugar level was determined; (2) The rats were allowed to rest for 20 minutes in a dark room; (3) A tracer (^{18}F-FDG, synthesized with Mini Tracer accelerator, 0.11 mci/kg dosage, PET-CT Center of the Experimental Animals Center of the No. 301 Chinese PLA General Hospital, Beijing, China) was injected *via* the tail vein; (4) The rats were allowed to rest for 40 minutes; (5) The rats were subjected to PET scans (Siemens, Germany). PET scans were performed on a Biograph Duo BGO scanner (Siemens). The images encompassed the whole brain and neck. The matrix size of the PET images was 128 × 128 × 63, and the format was ANALYZE 7.5.

PET image post-processing was performed using the pixel statistics analysis software SPM2, based on the Matlab platform (the Institute of High Energy Physics of the Chinese Academy of Sciences, Beijing, China). Pre-processing and data analysis were performed using our self-developed toolbox for voxel-wise analysis of rat brain images based on SPM8 (Welcome Department of Cognitive Neurology, London, UK), which comprised a FDG-PET rat brain template and atlas in Paxinos & Watson space (Nie et al., 2013). The images of all rats in the model, sham-point, ST36 and normal groups were pre-processed using the following main steps: (1) segmentation; (2) normalization; (3) smoothing.

Statistical analysis and image processing

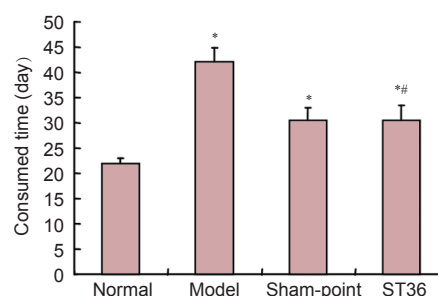Y-maze data were analyzed by one-way analysis of variance and

Figure 1 Learning and memory skills assessed by Y-maze test.
*$P < 0.05$, *vs.* normal group; #$P < 0.05$, *vs.* model group (mean ± SD, n = 15, one-way analysis of variance and the least significant difference test).

Table 1 Increased glucose metabolism in different brain regions in the normal group compared with the model group

Anatomical structures	Max_T	Peak coordinates (mm)		
		X	Y	Z
Right auditory cortex	4.18	6.45	5.30	−3.72
Right cingulate gyrus	4.85	0.10	3.11	2.04
Left dorsal thalamus_lateral nucleus group	4.24	−1.59	6.44	−2.04
Left hippocampus	3.86	−5.96	5.56	−4.92
Left midbrain_inferior colliculus	3.54	−2.85	4.95	−7.56
Left midbrain_tegmentum of midbrain	3.63	−2.84	5.56	−7.80
Right piriform cortex	3.77	4.13	8.31	0.36
Right prelimbic cortex	5.07	0.09	3.21	2.52
Left sensory cortex	3.89	−4.15	2.49	−0.36
Left striatum	5.11	−4.01	2.96	−0.60

T: *t*-value in the *t*-test.

the least significant difference test, and were expressed as the mean ± SD and processed with the Statistical Package for the Social Sciences version 13.0 software (SPSS, Chicago, IL, USA). A value of $P < 0.05$ was considered statistically significant.

Results

Effects of long-term acupuncture at ST36 on learning and memory abilities in AD rats

After acupuncture, the ST36 and sham-point groups displayed a significant improvement in learning and memory functions, evidenced by the reduction in the length of time required for training to achieve the learning criterion in the Y-maze test (**Figure 1**).

Effects of long-term acupuncture at ST36 on multi-regional brain activation in AD rats

Compared with the model group, the normal group exhibited a higher level of glycol metabolism in the right auditory cortex, right cingulate gyrus, left lateral nucleus group of the dorsal thalamus, left hippocampus, left inferior colliculus and tegmentum of the midbrain, right piriform cortex, right prelimbic cortex, left sensory cortex, and the left striatum (**Table 1** and **Figure 2**). Compared with the model group, the ST36 group exhibited a higher level of glycol metabolism in the left hippocampus, left infralimbic cortex, left medulla
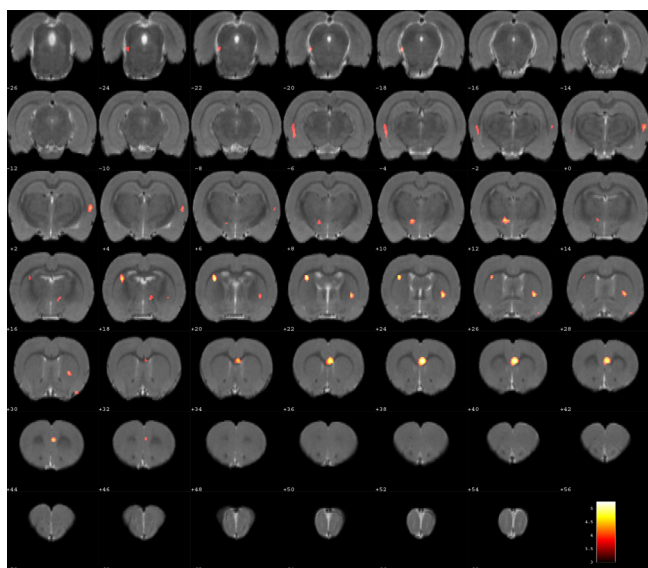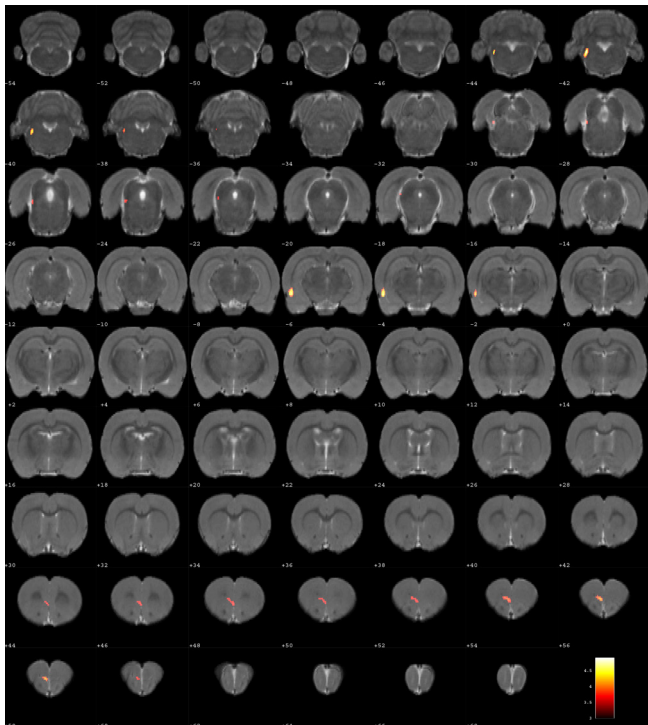
Figure 2 Changes in glucose metabolism in different brain regions in the normal group compared with the model group (coronal view).
The color (gradient shown in the vertical bar in the lower right) indicates the relative degree of glucose metabolism. A brighter color indicates higher metabolism. The numbers represent the coordinates of each virtual brain slice. Glucose metabolism in normal rats was relatively increased in the right auditory cortex, right cingulate gyrus, left lateral nucleus group of the dorsal thalamus, left hippocampus, left inferior colliculus and tegmentum of the midbrain, right piriform cortex, right prelimbic cortex, left sensory cortex, and the left striatum.

Figure 3 Changes in glucose metabolism in different brain regions in the *Zusanli* (ST36) group compared with the model group (coronal view).
Differences are color-coded. Glucose metabolism was relatively increased in the ST36 group in the left hippocampus, left infralimbic cortex, left medulla oblongata, left inferior colliculus of the midbrain, left olfactory cortex, left orbital cortex, left tegmentum of pons, and the left prelimbic cortex.
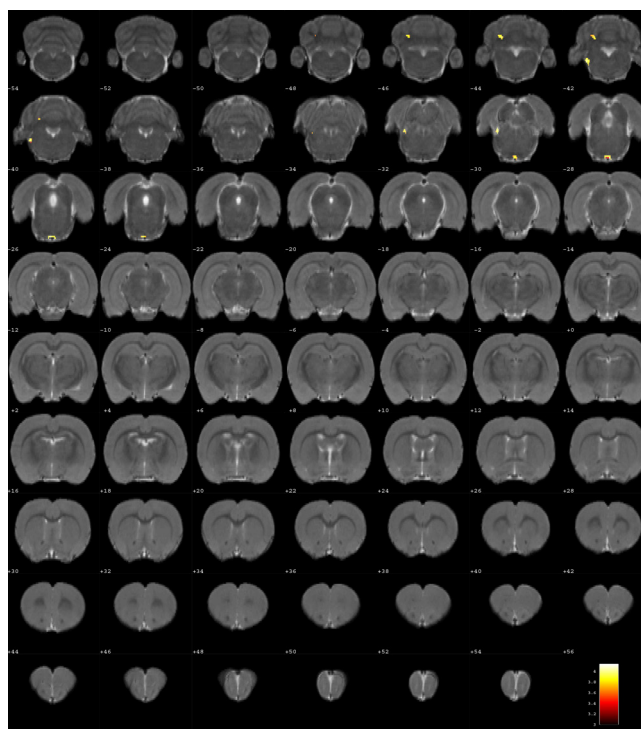

Figure 4 Changes in glucose metabolism in different brain regions in the *Zusanli* (ST36) group compared with the sham-point group (coronal view).
Differences are color-coded. Glucose metabolism in the ST36 group was relatively higher in the left anterior lobe, posterior lobe of the cerebellum, left basilar part of the pons and the left tegmentum of the pons.

Table 2 Increased glucose metabolism in different brain regions in the *Zusanli* (ST36) group compared with the model group

Anatomical structures	Max_T	Peak coordinates (mm)		
		X	Y	Z
Left hippocampus	3.98	−6.09	5.87	−5.16
Left infralimbic cortex	3.67	−0.46	4.29	3.24
Left medulla oblongata	4.62	−3.07	6.84	−10.92
Left midbrain_inferior colliculus	3.74	−2.98	4.67	−7.80
Left olfactory cortex	4.70	−6.36	6.25	−4.68
Left orbital cortex	4.10	−0.88	3.21	5.16
Left pontine_tegmentum of pons	3.96	−3.47	7.24	−10.68
Left prelimbic cortex	3.66	−0.72	3.98	3.24

T: *t*-value in the *t*-test.

Table 3 Increased glucose metabolism in different brain regions in the *Zusanli* (ST36) group compared with the sham-point group

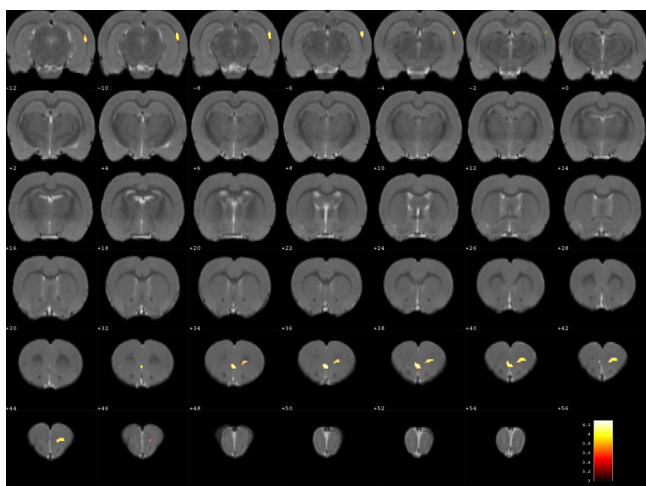| Anatomical structures	Max_T	Peak coordinates (mm)		
		X	Y	Z
Left cerebellum_anterior lobe	3.98	−2.40	3.96	−10.92
Left cerebellum_posterior lobe	3.90	−2.80	3.67	−11.16
Left pontine_basilar part	3.86	−0.84	9.49	−8.04
Left pontine_tegmentum of pons	3.94	−3.74	7.22	−10.68

T: *t*-value in the *t*-test.

Figure 5 Changes in glucose metabolism in different brain regions in the sham-point group compared with the model group (coronal view).
Differences are color-coded. Glucose metabolism in the sham-point group was relatively higher in the right auditory cortex, left infralimbic cortex, left orbital cortex, left prelimbic cortex and the right sensory cortex.
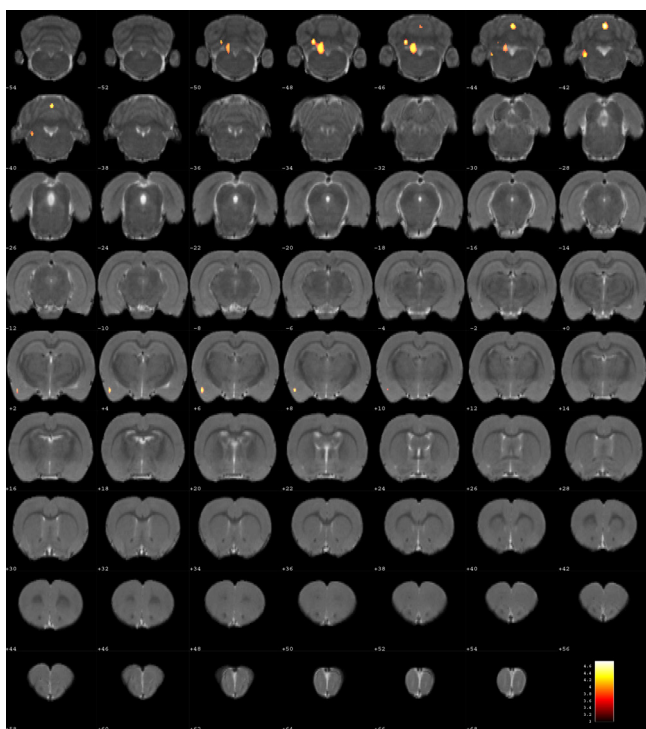

Figure 6 Changes in glucose metabolism in different brain regions in the *Zusanli* (ST36) group compared with the normal group (coronal view).
Differences are color-coded. Glucose metabolism in the ST36 group was relatively higher in the left amygdaloid body, right anterior lobe, left cerebellar nucleus, left posterior lobe of the cerebellum, left piriform cortex, and the left tegmentum of the pons.

Figure 7 Changes of in glucose metabolism in different brain regions in the sham-point group compared with the normal group (coronal view).
Differences are color-coded. Glucose metabolism was relatively higher in the sham-point group in the right anterior lobe, right posterior lobe of the cerebellum, left hippocampus, right infralimbic cortex, left superior colliculus of midbrain, right orbital cortex and the right visual cortex.

Table 4 Increased glucose metabolism in different brain regions in the sham-point group compared with the model group

Anatomical structures	Max_T	Peak coordinates (mm)		
		X	Y	Z
Right auditory cortex	3.91	6.07	3.48	–4.92
Left infralimbic cortex	3.51	–0.46	4.29	3.24
Left orbital cortex	4.29	–0.47	3.91	4.20
Left prelimbic cortex	3.79	–0.60	3.80	3.72
Right sensory cortex	3.76	5.93	3.14	–4.44

T: *t*-value in the *t*-test.

oblongata, left inferior colliculus of the midbrain, left olfactory cortex, left orbital cortex, left tegmentum of the pons, and the left prelimbic cortex (**Table 2** and **Figure 3**). Compared with the sham-point group, the ST36 group showed a higher level of glycol metabolism in the left anterior lobe and posterior lobe of the cerebellum, left basilar part of the pons,
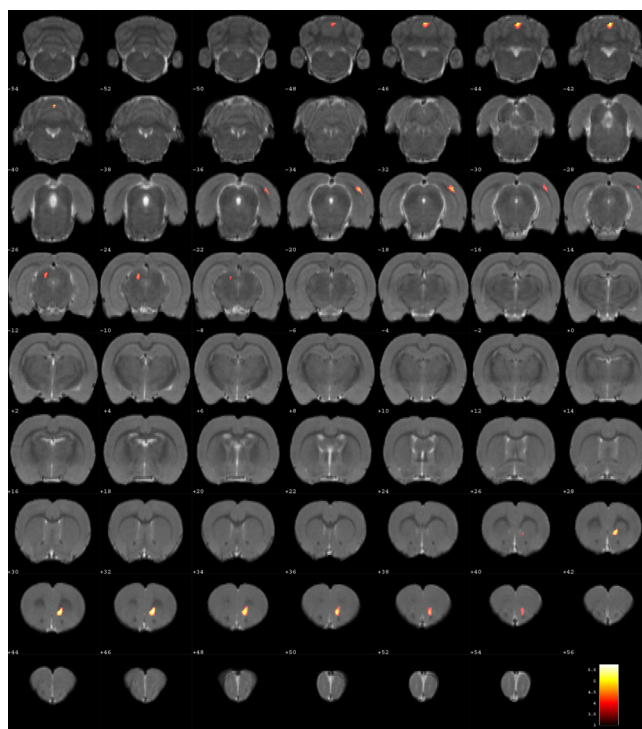and the left tegmentum of the pons (**Table 3** and **Figure 4**). Compared with the model group, the sham-point group showed a higher level of glycol metabolism in the right auditory cortex, left infralimbic cortex, left orbital cortex, left prelimbic cortex and right sensory cortex (**Table 4** and **Figure 5**). Compared with the normal group, the ST36 group showed a higher level of glycol metabolism in the left amygdaloid body, right anterior lobe, left cerebellar nucleus and left posterior lobe of the cerebellum, the left piriform cortex, and the left tegmentum of the pons (**Table 5** and **Figure 6**). Compared with the normal group, the sham-point group displayed a higher level of glycol metabolism in the right anterior lobe and right posterior lobe of the cerebellum, left hippocampus, right infralimbic cortex, left superior colliculus of the midbrain, right orbital cortex, and the right visual

Table 5 Increased glucose metabolism in different brain regions in the *Zusanli* (ST36) group compared with the normal group

Anatomical structures	Max_T	Peak coordinates (mm)		
		X	Y	Z
Left amygdaloid body	3.71	−5.58	7.75	−3.00
Right cerebellum_anterior lobe	4.73	0.14	2.48	−10.68
Left cerebellum_cerebellar nucleus	3.59	−1.86	5.35	−11.40
Left cerebellum_posterior lobe	4.12	−0.92	6.01	−11.64
Left piriform cortex	4.28	−5.85	7.74	−3.00
Left pontine_tegmentum of pons	3.50	−1.05	6.58	−11.64

T: *t*-value in the *t*-test.

Table 6 Increased glucose metabolism in different brain regions in the sham-point group compared with the normal group

Anatomical structures	Max_T	Peak coordinates (mm)		
		X	Y	Z
Right cerebellum_anterior lobe	5.12	0.14	2.04	−10.68
Right cerebellum_posterior lobe	3.63	0.29	2.30	−11.88
Left hippocampus	3.59	−1.41	3.07	−5.16
Right infralimbic cortex	4.83	0.61	4.50	3.24
Left midbrain_superior colliculus	3.85	−1.40	3.28	−5.88
Right orbital cortex	4.97	1.01	4.48	3.72
Right visual cortex	4.50	4.90	2.73	−7.08

T: *t*-value in the *t*-test.

cortex (**Table 6** and **Figure 7**).

Discussion

Our results demonstrate that long-term acupuncture treatment has therapeutic efficacy for AD. Rats in the ST36 group finished the Y-maze test in a shorter time compared with the sham-point and model groups, suggesting an improvement of symptoms. ^{18}F-FDG PET was applied in the study to provide insight into the underlying mechanisms. Memory disorder, one of the prominent features of AD, is reflected pathologically as a reduction in glucose metabolism in several brain regions of AD rats compared with the normal group. These regions included the hippocampus, the tegmentum of the midbrain, the prelimbic cortex, the auditory cortex, the striatum and the cingulate gyrus. ST36 is a key acupoint in acupuncture treatment for many brain diseases, especially AD. After needling at ST36, glucose metabolism was increased in brain regions in the left hippocampus and the left prelimbic cortex. These changes are evidence of a targeted effect of acupuncture on multiple brain areas. Needling at ST36 also stimulated other brain regions, including the left infralimbic cortex, the left medulla oblongata, the left olfactory cortex, the left orbital cortex and the left tegmentum of the pons. We speculate that these effects of acupuncture enhance brain function and ameliorate cognitive impairment, in line with the study by Wang et al. (2012).

In addition to cognitive impairment, a number of AD patients also suffer from behavioral and psychiatric symptoms, among which agitation and depression are the most common (Tsai et al., 2013). In our experiment, the orbital cortex, the medulla oblongata and the tegmentum of the pons were activated after needling at ST36. As a part of the prefrontal cortex, the orbital cortex is considered of vital importance in the control of emotions. When damaged, this control, especially the inhibition of impulsivity, can be perturbed (Kuo et al., 2015). AD patients can also exhibit disturbances in eating and circadian rhythms (Kai et al., 2015; Musiek et al., 2015), which are related to the medulla oblongata and the tegmentum of the pons. As AD progresses, some patients may experience motor system dysfunction, which is also associated with pontine activity (Lam et al., 2013; Takakusaki et al., 2016). In the present study, the left tegmentum of the pons was activated after needling at ST36 in both the normal and model groups, with a larger increase in the latter.

This suggests that acupuncture at ST36 may be effective for treating AD. Although studies on the effects of acupuncture on non-cognitive symptoms are lacking, acupuncture might produce an overall improvement in the disease.

The sham-point group shared some similarities with the ST36 group, compared with the model group, as both groups exhibited an upregulation of glucose metabolism of the left infralimbic cortex, left orbital cortex and left prelimbic cortex. The Y-maze test results were also similar among the sham-point and ST36 groups. One possible reason for these similarities is that ST36 and the sham-point are part of the same nerve segment (Ren et al., 2014). When needling at ST36 or the sham point, the brain regions connected with these nerve segments were activated. Furthermore, the locations of ST36 and the sham point are close, particularly in the rat. The brain regions activated in both the ST36 and sham-point groups included the left cerebellum and the left pons. Moreover, the sham-point stimulation activated the right auditory cortex and the right sensory cortex. Damage to the auditory cortex can be reflected in verbal episodic memory impairment in AD (Dhanjal et al., 2013). Therefore, an increase in metabolism could account for the targeted therapeutic effect of acupuncture. In addition, it is reported that nearly half of AD patients have hallucinations (Murray et al., 2014). This might be related to dysfunction of the sensory cortex. PET observation has not been previously reported for needling at the sham point for treating AD, and therefore requires further study.

This study has a couple of limitations. First, our AD model was generated by intraperitoneal injection of D-galactose combined with the injection of ibotenic acid into the basal nuclei. Other studies have used transgenic mice, which better mimic the most salient characteristics of AD. Second, we used only one acupoint. Acupuncture at multiple acupoints is generally required for clinical treatment. The therapeutic effectiveness of long-term acupuncture for treating AD involves three mechanisms: targeting the affected regions, compensation by other brain regions, and the targeted regulation of multiple regions. The latter appears to be the most important. Our study provides insight into the mechanisms underlying the beneficial effects of acupuncture for the treatment of AD.

References

Budni J, Pacheco R, Da Silva S, Garcez ML, Mina F, Bellettini-Santos T, de Medeiros J, Voss BC, Steckert AV, Valvassori Sda S, Quevedo J (2016) Oral administration of d-galactose induces cognitive impairments and oxidative damage in rats. Behav Brain Res 302:35-43.

Dhanjal NS, Warren JE, Patel MC, Wise RJ (2013) Auditory cortical function during verbal episodic memory encoding in Alzheimer's disease. Ann Neurol 73:294-302.

Dukart J, Mueller K, Villringer A, Kherif F, Draganski B, Frackowiak R, Schroeter ML (2013) Relationship between imaging biomarkers, age, progression and symptom severity in Alzheimer's disease. Neuroimage Clin 3:84-94.

Hu Y (2003) Acupoint location for experimental animals. Beijing: China Agriculture Press.

Kai K, Hashimoto M, Amano K, Tanaka H, Fukuhara R, Ikeda M (2015) Relationship between eating disturbance and dementia severity in patients with Alzheimer's disease. PLoS One doi:10.1371/journal.pone.0133666.

Karthick C, Periyasamy S, Jayachandran KS, Anusuyadevi M (2016) Intrahippocampal administration of ibotenic acid induced cholinergic dysfunction via NR2A/NR2B expression: implications of resveratrol against alzheimer disease pathophysiology. Front Mol Neurosci 9:28.

Kuo MF and Nitsche MA (2015) Exploring prefrontal cortex functions in healthy humans by transcranial electrical stimulation. Neurosci Bull 31:198-206.

Lai X, Ren J, Lu Y, Cui S, Chen J, Huang Y, Tang C, Shan B, Nie B (2015) Effects of acupuncture at HT7 on glucose metabolism in a rat model of Alzheimer's disease: an ^{18}F-FDG-PET study. Acupunct Med doi:10.1136/acupmed-2015-010865.

Lam B, Masellis M, Freedman M, Stuss DT, Black SE (2013) Clinical, imaging, and pathological heterogeneity of the Alzheimer's disease syndrome. Alzheimers Res Ther 5:1.

Li W, Kong LH, Wang H, Shen F, Wang YW, Zhou H, Sun GJ (2016) High-frequency electroacupuncture evidently reinforces hippocampal synaptic transmission in Alzheimer's disease rats. Neural Regen Res 11:801-806.

Lin Y, Ji F, Huang GR, Li P (2013) Our considerations about non-acupoint selection for experimental studies in rats. Zhen Ci Yan Jiu 38:334-338.

Lu Y, Huang Y, Tang C, Shan B, Cui S, Yang J, Chen J, Lin R, Xiao H, Qu S, Lai X (2014) Brain areas involved in the acupuncture treatment of AD model rats: a PET study. BMC Complement Altern Med 14:178.

Lu Y, Ren J, Cui S, Chen J, Huang Y, Tang C, Shan B, Nie B, Lai X (2015) Cerebral glucose metabolism assessment in rat models of alzheimer's disease: an 18F-FDG-PET study. Am J Alzheimers Dis Other Demen 31:333-340.

Murray PS, Kumar S, Demichele-Sweet MA, Sweet RA (2014) Psychosis in Alzheimer's disease. Biol Psychiatry 75:542-552.

Musiek ES, Xiong DD and Holtzman DM (2015) Sleep, circadian rhythms, and the pathogenesis of Alzheimer disease. Exp Mol Med doi:10.1038/emm.2014.121.

Nie B, Chen K, Zhao S, Liu J, Gu X, Yao Q, Hui J, Zhang Z, Teng G, Zhao C, Shan B (2013) A rat brain MRI template with digital stereotaxic atlas of fine anatomical delineations in paxinos space and its automated application in voxel-wise analysis. Hum Brain Mapp 34:1306-1318.

Ren BB, Yu Z, Wang YL, Xu B (2014) Regulatory effect of electroacupuncture on heart and stomach of rats. Zhongguo Zhong Xi Yi Jie He Za Zhi 34:1212-1215.

Roy K, Pepin LC, Philiossaint M, Lorius N, Becker JA., Locascio JJ, Rentz DM, Sperling RA, Johnson KA, Marshall GA (2014) Regional fluorodeoxyglucose metabolism and instrumental activities of daily living across the Alzheimer's disease spectrum. J Alzheimers Dis 42:291-300.

Simoncini M, Gatti A, Quirico PE, Balla S, Capellero B, Obialero R, D'Agostino S, Sandri N, Pernigotti LM (2015) Acupressure in insomnia and other sleep disorders in elderly institutionalized patients suffering from Alzheimer's disease. Aging Clin Exp Res 27:37-42.

Tahmasian M, Pasquini L, Scherr M, Meng C, Forster S, Mulej Bratec S, Shi K, Yakushev I, Schwaiger M, Grimmer T, Diehl-Schmid J, Riedl V, Sorg C, Drzezga A (2015) The lower hippocampus global connectivity, the higher its local metabolism in Alzheimer disease. Neurology 84:1956-1963.

TakakusakiK, Chiba R, Nozu T, Okumura T (2016) Brainstem control of locomotion and muscle tone with special reference to the role of the mesopontine tegmentum and medullary reticulospinal systems. J Neural Transm (Vienna) 123:695-729.

Tsai CF, Hung CW, Lirng JF, Wang SJ, Fuh JL (2013) Differences in brain metabolism associated with agitation and depression in Alzheimer's disease. East Asian Arch Psychiatry 23:86-90.

Wang Z, Nie B, Li D, Zhao Z, Han Y, Song H, Xu J, Shan B, Lu J, Li K (2012) Effect of acupuncture in mild cognitive impairment and Alzheimer disease: a functional MRI study. PLoS One doi:10.1371/journal.pone.0042730.

Xiao N, Zhang J, Zhou M, Wei Z, Wu X, Dai X, Zhu Y, Chen X (2015) Reduction of glucose metabolism in olfactory bulb is an earlier alzheimer's disease-related biomarker in 5XFAD mice. Chin Med J (Engl) 128:2220-2227.

Zhang S, Huang XY, Liu S, Li YJ, Zhao JC (2016) Effects of amyloid-beta 25-35 on expression of synapse-associated proteins in PC12 neurons Effects of amyloid-beta 25-35 on expression of synapse-associated proteins in PC12 neurons. Zhongguo Zuzhi Gongcheng Yanjiu 20:224-229.

Zhong Z, Qu Z, Wang N, Wang J, Xie Z, Zhang F, Zhang W, Lu Z (2005a) Protective effects of Panax notoginseng saponins against pathological lesion of cholinergic neuron in rat model with Alzheimer's disease. Zhong Yao Cai 28:119-122.

Zhong Z, Qu Z, Wang N, Zhang F, Zhang W, Lu U (2005b) Effects of the Panax notoginseng saponins on the level of synaptophysin protein in brain in rat model with lesion of Meynert. Zhongguo Zhong Yao Za Zhi 30:913-915.

Zhou J, Peng W, Xu M, Li W, Liu Z (2015) The effectiveness and safety of acupuncture for patients with Alzheimer disease: a systematic review and meta-analysis of randomized controlled trials. Medicine (Baltimore) 94:e933.

Copyedited by Patel B, Wysong S, Wang J, Li CH, Qiu Y, Song LP, Zhao M